

General corner states in 2D SSH model with intracelluar next-nearest-neighbour hopping

Xun-Wei Xu,^{1,*} Yu-Zeng Li,¹ Zheng-Fang Liu,¹ and Ai-Xi Chen^{2,1,†}

¹*Department of Applied Physics, East China Jiaotong University, Nanchang, 330013, China*

²*Department of Physics, Zhejiang Sci-Tech University, Hangzhou 310018, China*

(Dated: March 31, 2020)

We investigate corner states in a photonic two-dimensional (2D) Su-Schrieffer-Heeger (SSH) model on a square lattice with zero gauge flux. By considering intracelluar next-nearest-neighbor (NNN) hoppings, we discover a broad class of corner states in the 2D SSH model, and show that they are robust against certain fabrication disorders. Moreover, these corner states are located around the corners, but not at the corner points, so we refer to them as general corner states. We analytically identify that the general corner states are induced by the intracelluar NNN hoppings (long-range interactions) and split off from the edge-state bands. Our work show a simple way to induce unique corner states by the long-range interactions, and offers opportunities for designing novel photonic devices.

I. INTRODUCTION

Topological photonics is a rapidly emerging research field based on topological band theory [1], inspired by topological phases and phase transitions in solid-state electron systems. It provides us the geometrical and topological ideas to design and control the behavior of photons, leading to interesting phenomena such as the properties of against backscattering and robust to defects and disorders. To highlight one important example, topologically protected photonic modes have been used both theoretically and experimentally to demonstrate topological insulator laser in a topological edge state [2–6]. In recent years, a class of interesting topological phases have been introduced in photonic topological systems, such as topological phases of non-Hermitian systems [7–24], nonlinear-photonic topological phase [25–31], topological quantum matter in synthetic dimensions [32–39], and higher-order topological insulators (HOTIs) [40–44].

In contrast to conventional (first-order) topological states, higher-order topological (HOT) states two or more dimensions lower than the system are hosted in HOTIs [45–50]. To date the HOT states have been implemented in many different types of photonic lattices, such as the honeycomb lattice [51–53], the Kagome lattice [54–57], and the square lattice [58–66].

In this paper, we will focus on HOT states (i.e., corner states) in two-dimensional (2D) Su-Schrieffer-Heeger (SSH) model on a square lattice. It has been demonstrated experimentally that the standard 2D SSH model can not support robust corner states for the zero-energy modes are located in the bulk band [61]. To observe topologically protected corner state in the photonic 2D SSH model, a synthetic magnetic flux of π per plaquette, i.e., negative coupling, was proposed theoretically [40]

and demonstrated experimentally [58–62] in some recent works. Besides, topologically protected corner states also have been observed in the band gap in 2D dielectric photonic crystals on SSH model [63–66], which can be understood by considering the higher-order couplings such as the next-nearest-neighbor (NNN) coupling between the dielectric rods which inevitably break the chiral symmetry. However, the effects of NNN coupling on topological phases is still an open question at the moment.

Here, we will investigate how to observe corner states in the 2D SSH model with intracelluar NNN hopping in tight-binding representation. We note that the effects of NNN coupling on topological phases have been explored in bipartite lattices for reconfigurable topological phases [67] and topological defect states [68]. Nevertheless, we find that intracelluar NNN coupling can induced new corner states in the 2D SSH model. Different from the conventional corner states observed before, the intracelluar NNN coupling induced corner states appear around the corners but not at the corner points, so we refer to them as general corner states. We also note that these general corner states are similar to the type II corner states observed in photonic kagome crystals very recently [69]. However, we show that the general corner states are a broad class of corner states splitting from the topological edge-state bands with the increasing of the intracelluar NNN coupling, not just two type II corner states observed in Ref. [69]. Moreover, the general corner states can be understood intuitively by the separate model fragments of the 2D SSH model. Our work broadens the concept of corner states and provides new ideas for designing novel photonic devices.

II. 2D SSH MODEL

We consider a photonic 2D SSH model with $N \times M$ unit cells, as shown in Fig. 1. There are four modes A , B , C , and D in one unit cell with eigenfrequencies ω_a , ω_b , ω_c , and ω_d , where γ and λ are the amplitudes of

* davidxu0816@163.com

† aixichen@zstu.edu.cn

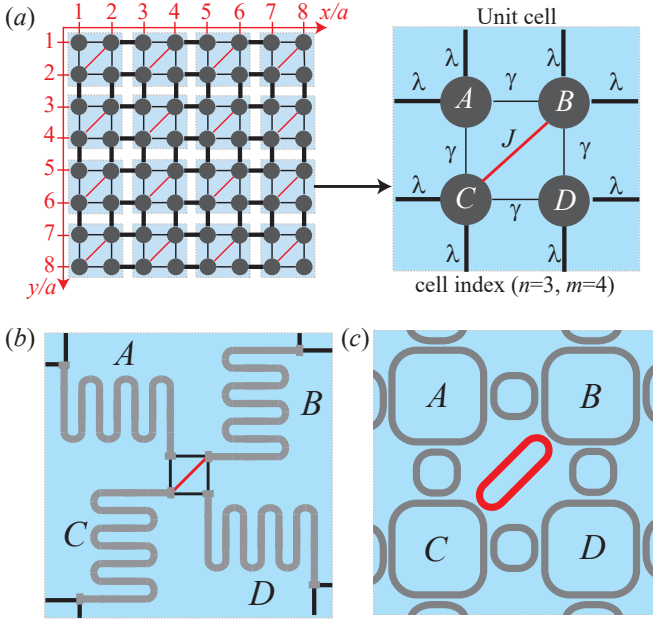


FIG. 1. (Color online) (a) Schematic of a photonic 2D SSH model on a square lattice. There are four modes (A , B , C , and D) in one unit cell with lattice constant $2a$ and the amplitudes of intracelluar and intercelluar nearest-neighbor hoppings are γ and λ , respectively. The red oblique lines represent intercelluar next-nearest-neighbor (NNN) hoppings in unit cells with strength J . The possible realistic physical systems to implement one unit cell of the photonic 2D SSH model: (b) network of coupled superconducting transmission line resonators [70–72] and (c) 2D lattice of nanophotonic silicon ring resonators [61].

intracelluar and intercelluar (nearest-neighbor) hoppings, J is the strength of the intracelluar NNN hopping (long-range interaction) in unit cells. Different from the model studied in Refs. [58–61], where a synthetic magnetic flux of π per plaquette, i.e., negative coupling, is applied to the square lattices, here all the hoppings γ , λ , and J are positive, that is, it is a 2D SSH model on a square lattice with zero gauge flux. In the rotating frame with respect to the frequency of all the optical modes $\omega_a = \omega_b = \omega_c = \omega_d = \omega$, the Hamiltonian for the 2D SSH model is described by ($\hbar = 1$)

$$\begin{aligned}
 H = & \sum_{n=1}^N \sum_{m=1}^M [\gamma(a_{n,m} + d_{n,m})(b_{n,m}^\dagger + c_{n,m}^\dagger) + Jb_{n,m}c_{n,m}^\dagger] \\
 & + \sum_{n=2}^N \sum_{m=1}^M [\lambda(a_{n,m}c_{n-1,m}^\dagger + b_{n,m}d_{n-1,m}^\dagger)] \\
 & + \sum_{n=1}^N \sum_{m=2}^M [\lambda(a_{n,m}b_{n,m-1}^\dagger + c_{n,m}d_{n,m-1}^\dagger)] \\
 & + \text{H.c.}, \quad (1)
 \end{aligned}$$

where (n, m) are integers indexing the lattice sites. To detect the robustness of the system, in the numerical calculations, we will consider the disorder effect of the

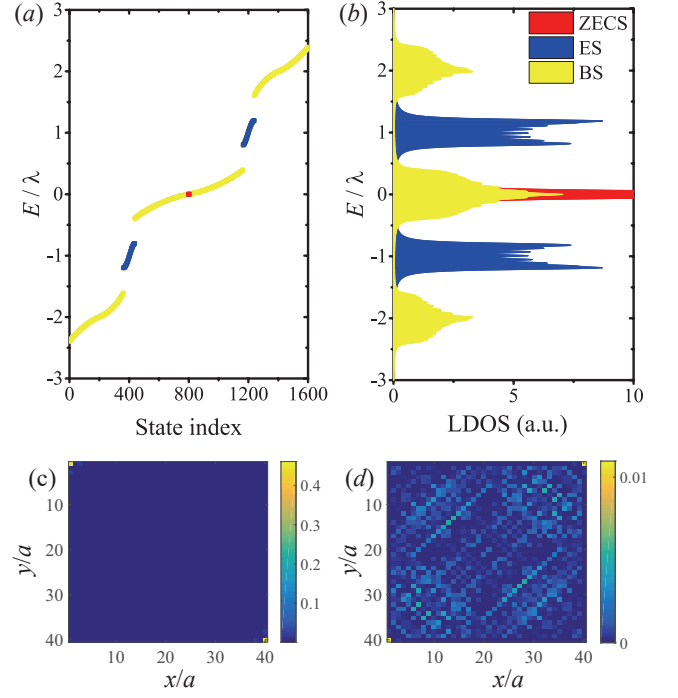


FIG. 2. (Color online) (a) Energy spectrum for a 2D SSH model with a 20×20 array of unit cells, with $\gamma = \lambda/5$ and $J = 0$. (b) Corresponding local density of states (LDOS) with $\kappa = \lambda/20$. The blue bands denote the the topological edge states (ES) of the lattice, the bulk states (BS) are depicted by yellow bands and the four degenerate zero-energy corner states (ZECS) appear at zero energy with no bandgap (highlighted in red). The field profiles of the corner states without disorder in (c) and with disorder $\epsilon \in [-\lambda/100, \lambda/100]$ in (d).

parameters with $\omega + \epsilon$, $\gamma + \epsilon$, $\lambda + \epsilon$, and $J + \epsilon$, where $\epsilon \in [-\lambda/100, \lambda/100]$ is randomly distributed.

The 2D SSH model can be implemented in a network of coupled superconducting transmission line resonators [70–72], as schematically shown in Fig. 1(b). Resonators b and c are connected by an auxiliary capacitor (in red) as shown in Fig. 1(c). The 2D SSH model can also be realized using a 2D lattice of nanophotonic silicon ring resonators as reported in Ref. [61]. These ring- c and ring- d can be coupled to each other using an auxiliary ring (in red) as shown in Fig. 1(d).

III. GENERAL CORNER STATES

First of all, let us review the corner state in the 2D SSH model without intracelluar NNN hopping, i.e., $J = 0$. The energy spectrum for a 2D SSH model without intracelluar NNN hopping is shown in Fig. 2(a). There are five bands, two (in blue) are edge-state bands and three (in yellow) are bulk-state bands. The energy bands can be reflected in the local density of states (LDOS), as shown in Fig. 2(b). The LDOS can be calculation based on the Green function in frequency space (see Ref. [73] or

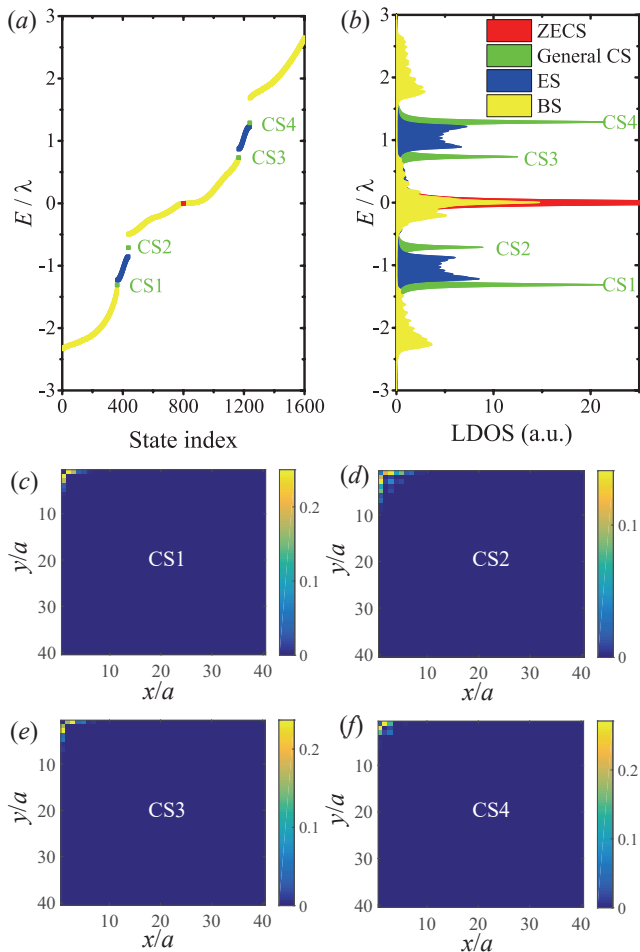


FIG. 3. (Color online) (a) Energy spectrum for a 2D SSH model with a 20×20 array of unit cells, with $\gamma = \lambda/5$ and $J = \lambda/2$. (b) Corresponding LDOS with $\kappa = \lambda/20$. The general corner states (CS) (CS1-CS4, highlighted in green) appear in the band gaps between the edge and bulk bands. The field profiles of the general corner states CS1-CS4 in (c)-(f) with disorder $\epsilon \in [-\lambda/100, \lambda/100]$.

Appendix A), and the photonic LDOS is experimentally accessible via reflection/transmission measurements.

Figure 2(c) shows that the 2D SSH model with zero gauge flux hosts zero-energy states localized at the corners, similar to those of the 2D SSH model with π gauge flux [58–61]. However, there is no bandgap at zero energy in the energy spectrum of the model as shown in Fig. 2(b), which indicates that this zero-energy corner states are not topologically protected and are susceptible to the fabrication disorders. Consequently, the disorder, which is a very common phenomenon in the experimental set-ups, can easily couple these corner states to the bulk states located near zero energy, as shown in the field profiles of the zero-energy corner states with disorder $\epsilon \in [-\lambda/100, \lambda/100]$ in Fig. 2(d). These agree with a recently experimental results [61]. As this type of zero-energy corner states are susceptible to the fabrica-

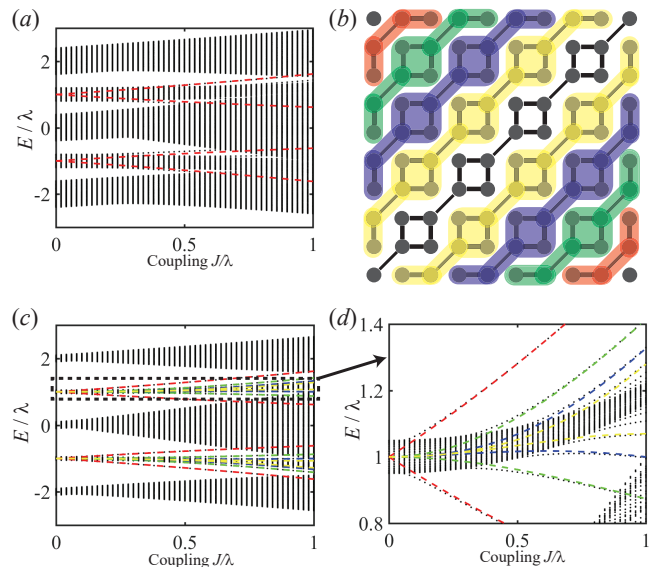


FIG. 4. (Color online) (a) Energy spectrum of a 2D SSH model with varying intercellular NNN hopping J/λ , with $\gamma = \lambda/5$. (b) Illustration of coupling between modes around the corners forming general corner states with $\gamma = 0$. (c) Energy spectrum of a 2D SSH model with varying intercellular NNN hopping J/λ , with $\gamma = \lambda/20$. (d) Enlarged section of (c) showing the emergence of more corner states from the bands of edge states as J increases. The colored (red, green, blue, yellow) dashed lines show the analytical result for the energies of corner states obtained with modes around the corners highlighted in the same color (red, green, blue, yellow) in (b).

tion disorders and appear even in the absence of intracellular NNN hoppings, we will do not explore it in the following.

Next, we demonstrate that new corner states can be induced by the intracellular NNN hopping, even if there is no gauge flux through the lattice of the 2D SSH model. As shown in the energy spectrum [Fig. 3(a)] and LDOS [Fig. 3(b)], besides the corner states at zero energy (in red), there are four double degenerate corner states CS1-CS4 (highlighted in green) appear in the band gaps between the edge and bulk bands. Similar corner states have been observed in a 2D topological photonic crystal with kagome lattice very recently [69].

Here, we analyze the characteristics of the new corner states with the field profiles shown in Fig. 3(c)-3(f). (i) Different from the conventional corner states observed before, the new corner states are localized around the corners, but not at the four corner points $(x/a, y/a) = \{(1, 1), (1, 2M), (2N, 1), (2N, 2M)\}$. The highest values of the field profiles appear around the points $(x/a, y/a) = \{(1, 2), (1, 3), (2, 1), (3, 1)\}$ or $(x/a, y/a) = \{(2N-1, 2M), (2N-2, 2M), (2N, 2M-1), (2N, 2M-2)\}$ (not shown in the figures). Thus we refer to these new corner states as general corner states. (ii) The field profiles show that the general corner states are robust to random noises. This point is also evident in the energy

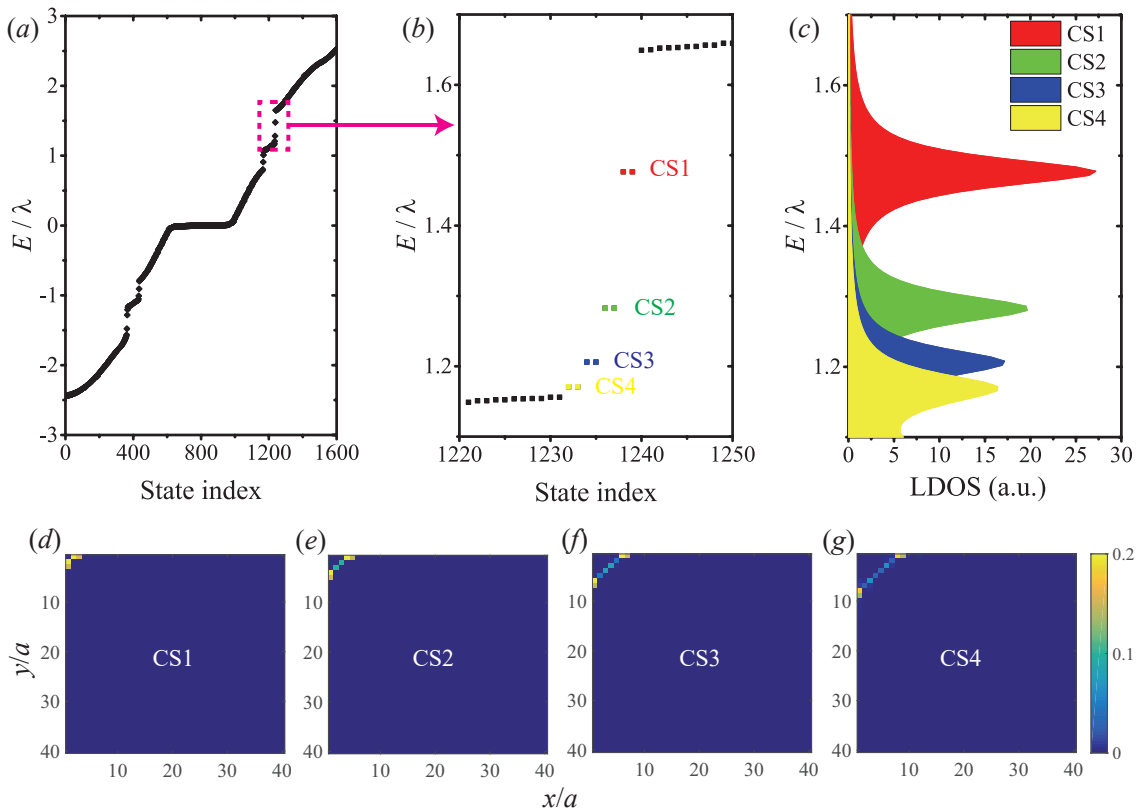


FIG. 5. (Color online) (a) Energy spectrum for a 2D SSH model with a 20×20 array of unit cells, with $\gamma = \lambda/20$ and $J = 0.8\lambda$. (b) Enlarged section of (a) showing four general corner states: CS1-CS4. (c) LDOS of the general corner states CS1-CS4 with $\kappa = \lambda/20$. (d)-(g) Corresponding field profiles of the corner states CS1-CS4 with disorder $\epsilon \in [-\lambda/100, \lambda/100]$.

spectrum and LDOS of the system, where the general corner states are separated from the edge and bulk bands [Figs. 3(a) and 3(b)].

To reveal the origin of general corner states, the energy spectrum of a 2D SSH model are plotted with varying intracelluar NNN hopping J/λ in Fig. 4(a). It was obvious that, the general corner states split off from the edge-state bands. The general corner states can be understood from the model in the case of $\gamma = 0$ as shown in Fig. 4(b), where the 2D SSH model has been divided into separate model fragments highlighted in different colors. The red dashed lines in Fig. 4(a) show the analytical result for the energies of corner states obtained with modes around the corners highlighted in red, which are agree with the energy spectrum of general corner states and the subtle difference are induced by the intracelluar hopping γ .

To show the general corner states induced by the other separate model fragments highlighted in different colors, the energy spectrum of a 2D SSH model with $\gamma = \lambda/20$

are plotted as a function of J/λ in Figs. 4(c) and 4(d). Interestingly, more general corner states (in different colors) split off from the edge-state bands with the increase of intracelluar NNN hopping J/λ . The energy of the general corner states are agree well with analytical results (the red, green, blue, and yellow dashed lines) obtained with modes around the corners highlighted in the same color (red, green, blue, yellow) in Fig. 4(b).

To further explore the characteristics of the general corner states, the energy spectrum for a 2D SSH model are shown in Figs. 5(a) and 5(b) with $\gamma = \lambda/20$ and $J = 0.8\lambda$. There are four double degenerate corner states CS1-CS4 appear in the band gap between the edge and bulk bands. These general corner states can be observed by the LDOS of the system as shown in Fig. 5(c). The corresponding field profiles of the general corner states are shown in Figs. 5(d)-5(g), which agree well with the separate model fragments in Fig. 4(b).

IV. CONCLUSIONS

In conclusion, we have demonstrated that the 2D SSH model on a square lattice without gauge flux can support

robust general corner states by considering the intracelluar NNN hoppings. We have analytically determined that the intracelluar NNN hoppings can result in the for-

mation of a broad class of general corner states, which can be understood intuitively by the separate model fragments of the 2D SSH model. We believe that our work opens important directions in inducing unique corner states by the intracelluar NNN hoppings (long-range interactions), and offering possibilities to control photons in novel ways.

Acknowledgement

X.-W.X. was supported by the Key Program of Natural Science Foundation of Jiangxi Province, China under Grant No. 20192ACB21002, and the National Natu-

ral Science Foundation of China (NSFC) under Grant No. 11604096. Z.-F.L. is supported by NSFC under Grant No. 11864012. A.-X.C. is supported by NSFC under Grant No. 11775190.

Appendix A: Calculation of the local density of states (LDOS)

Substituting the Hamiltonian (1) into the Heisenberg equation and taking into account the damping of the modes with damping rate κ and the corresponding quantum noises, we get the quantum Langevin equations (QLEs) for the operators in the unit cell with cell index (n, m) as:

$$i\frac{d}{dt}a_{n,m} = -i\frac{\kappa}{2}a_{n,m} + \gamma(b_{n,m} + c_{n,m}) + \lambda(b_{n,m-1} + c_{n-1,m}) + i\sqrt{\kappa}a_{n,m}^{(\text{in})}, \quad (\text{A1})$$

$$i\frac{d}{dt}b_{n,m} = -i\frac{\kappa}{2}b_{n,m} + \gamma(a_{n,m} + d_{n,m}) + \lambda(a_{n,m+1} + d_{n-1,m}) + Jc_{n,m} + i\sqrt{\kappa}b_{n,m}^{(\text{in})}, \quad (\text{A2})$$

$$i\frac{d}{dt}c_{n,m} = -i\frac{\kappa}{2}c_{n,m} + \gamma(a_{n,m} + d_{n,m}) + \lambda(a_{n+1,m} + d_{n,m-1}) + Jb_{n,m} + i\sqrt{\kappa}c_{n,m}^{(\text{in})}, \quad (\text{A3})$$

$$i\frac{d}{dt}d_{n,m} = -i\frac{\kappa}{2}d_{n,m} + \gamma(b_{n,m} + c_{n,m}) + \lambda(b_{n+1,m} + c_{n,m+1}) + i\sqrt{\kappa}d_{n,m}^{(\text{in})}, \quad (\text{A4})$$

where $q_{n,m}^{(\text{in})}$ ($q = a, b, c, d$) is the input quantum noise operators.

In order to calculate LDOS numerically in a finite system with $N \times M$ unit cells, the QLEs can be concisely expressed as

$$i\frac{dC}{dt} = AC + i\sqrt{\kappa}C_{\text{in}}, \quad (\text{A5})$$

where $C = (\dots, a_l, b_l, c_l, d_l, \dots)^T$ and $C_{\text{in}} = (\dots, a_l^{(\text{in})}, b_l^{(\text{in})}, c_l^{(\text{in})}, d_l^{(\text{in})}, \dots)^T$ are $4NM$ -dimensional vectors with the cell index $l = (n, m)$, and A is the

$4NM \times 4NM$ coefficient matrix. The Green function for photons with relative energy E is given by

$$G = \frac{1}{E - A}. \quad (\text{A6})$$

The LDOS is determined by

$$\rho(E, l_q) = -2\text{Im}G(E, l_q, l_q) \quad (\text{A7})$$

with subscript $q = a, b, c, d$.

-
- [1] T. Ozawa, H. M. Price, A. Amo, N. Goldman, M. Hafezi, L. Lu, M. C. Rechtsman, D. Schuster, J. Simon, O. Zeitlinger, and I. Carusotto, *Rev. Mod. Phys.* **91**, 015006 (2019).
- [2] B. Bahari, A. Ndao, F. Vallini, A. El Amili, Y. Fainman, and B. Kanté, *Science* **358**, 636 (2017).
- [3] G. Harari, M. A. Bandres, Y. Lumer, M. C. Rechtsman, Y. D. Chong, M. Khajavikhan, D. N. Christodoulides, and M. Segev, *Science* **359**, 1230 (2018).
- [4] M. A. Bandres, S. Wittek, G. Harari, M. Parto, J. Ren, M. Segev, D. N. Christodoulides, and M. Khajavikhan, *Science* **359**, 1231 (2018).
- [5] Y. Zeng, U. Chattopadhyay, B. Zhu, B. Qiang, J. Li, Y. Jin, L. Li, A. G. Davies, E. H. Linfield, B. Zhang, Y. Chong, and Q. J. Wang, *Nature* **578**, 246 (2020).
- [6] W. Zhang, X. Xie, H. Hao, J. Dang, S. Xiao, S. Shi, H. Ni, Z. Niu, C. Wang, K. Jin, X. Zhang, and X. Xu, [arXiv:2002.06513](https://arxiv.org/abs/2002.06513) [physics.optics].
- [7] B. Zhen, C. W. Hsu, Y. Igarashi, L. Lu, I. Kaminer, A. Pick, S.-L. Chua, J. D. Joannopoulos, and M. Soljačić,

- Nature* **525**, 354 (2015).
- [8] H. Zhao, X. Qiao, T. Wu, B. Midya, S. Longhi, and L. Feng, *Science* **365**, 1163 (2019).
- [9] S. Malzard, C. Poli, and H. Schomerus, *Phys. Rev. Lett.* **115**, 200402 (2015).
- [10] S. Weimann, M. Kremer, Y. Plotnik, Y. Lumer, S. Nolte, K. Makris, M. Segev, M. C. Rechtsman, and A. Szameit, *Nature Materials* **16**, 433 (2016).
- [11] T. E. Lee, *Phys. Rev. Lett.* **116**, 133903 (2016).
- [12] Y. Xu, S.-T. Wang, and L.-M. Duan, *Phys. Rev. Lett.* **118**, 045701 (2017).
- [13] F. K. Kunst, E. Edvardsson, J. C. Budich, and E. J. Bergholtz, *Phys. Rev. Lett.* **121**, 026808 (2018).
- [14] S. Yao and Z. Wang, *Phys. Rev. Lett.* **121**, 086803 (2018).
- [15] H. Shen, B. Zhen, and L. Fu, *Phys. Rev. Lett.* **120**, 146402 (2018).
- [16] Z. Gong, Y. Ashida, K. Kawabata, K. Takasan, S. Higashikawa, and M. Ueda, *Phys. Rev. X* **8**, 031079 (2018).
- [17] T. Liu, Y.-R. Zhang, Q. Ai, Z. Gong, K. Kawabata, M. Ueda, and F. Nori, *Phys. Rev. Lett.* **122**, 076801 (2019).
- [18] C. H. Lee, L. Li, and J. Gong, *Phys. Rev. Lett.* **123**, 016805 (2019).
- [19] C. Yin, H. Jiang, L. Li, R. Lü, and S. Chen, *Phys. Rev. A* **97**, 052115 (2018).
- [20] W. Hu, H. Wang, P. P. Shum, and Y. D. Chong, *Phys. Rev. B* **95**, 184306 (2017).
- [21] K. Kawabata, K. Shiozaki, and M. Ueda, *Phys. Rev. B* **98**, 165148 (2018).
- [22] V. M. Martinez Alvarez, J. E. Barrios Vargas, and L. E. F. Foa Torres, *Phys. Rev. B* **97**, 121401 (2018).
- [23] L. Jin and Z. Song, *Phys. Rev. B* **99**, 081103 (2019).
- [24] C. H. Lee and R. Thomale, *Phys. Rev. B* **99**, 201103 (2019).
- [25] J. Koch, A. A. Houck, K. L. Hur, and S. M. Girvin, *Phys. Rev. A* **82**, 043811 (2010).
- [26] Y. Lumer, Y. Plotnik, M. C. Rechtsman, and M. Segev, *Phys. Rev. Lett.* **111**, 243905 (2013).
- [27] P. Roushan, C. Neill, A. Megrant, Y. Chen, R. Babbush, R. Barends, B. Campbell, Z. Chen, B. Chiaro, A. Dunsworth, A. Fowler, E. Jeffrey, J. Kelly, E. Lucero, J. Mutus, P. J. J. O'Malley, M. Neeley, C. Quintana, D. Sank, A. Vainsencher, J. Wenner, T. White, E. Kapit, H. Neven, and J. Martinis, *Nature Physics* **13**, 146 (2016).
- [28] D. Leykam and Y. D. Chong, *Phys. Rev. Lett.* **117**, 143901 (2016).
- [29] Y. Hadad, A. B. Khanikaev, and A. Alù, *Phys. Rev. B* **93**, 155112 (2016).
- [30] X. Zhou, Y. Wang, D. Leykam, and Y. D. Chong, *New Journal of Physics* **19**, 095002 (2017).
- [31] R. Chaunsali and G. Theocharis, *Phys. Rev. B* **100**, 014302 (2019).
- [32] X.-W. Luo, X. Zhou, C.-F. Li, J.-S. Xu, G.-C. Guo, and Z.-W. Zhou, *Nature Communications* **6**, 7704 (2015).
- [33] X.-F. Zhou, X.-W. Luo, S. Wang, G.-C. Guo, X. Zhou, H. Pu, and Z.-W. Zhou, *Phys. Rev. Lett.* **118**, 083603 (2017).
- [34] L. Yuan, Q. Lin, M. Xiao, and S. Fan, *Optica* **5**, 1396 (2018).
- [35] T. Ozawa and H. M. Price, *Nature Reviews Physics* **1**, 349 (2019).
- [36] E. Lustig, S. Weimann, Y. Plotnik, Y. Lumer, M. Bandres, A. Szameit, and M. Segev, *Nature* **567**, 356 (2019).
- [37] A. Dutt, M. Minkov, and S. Fan, (2019), [arXiv:1911.11310](https://arxiv.org/abs/1911.11310) [[cond-mat.mes-hall](https://arxiv.org/abs/1911.11310)].
- [38] A. Dutt, Q. Lin, L. Yuan, M. Minkov, M. Xiao, and S. Fan, *Science* **367**, 59 (2020).
- [39] W. Zhang and X. Zhang, [arXiv:1906.02967](https://arxiv.org/abs/1906.02967) [[physics.optics](https://arxiv.org/abs/1906.02967)].
- [40] W. A. Benalcazar, B. A. Bernevig, and T. L. Hughes, *Science* **357**, 61 (2017).
- [41] J. Langbehn, Y. Peng, L. Trifunovic, F. von Oppen, and P. W. Brouwer, *Phys. Rev. Lett.* **119**, 246401 (2017).
- [42] Z. Song, Z. Fang, and C. Fang, *Phys. Rev. Lett.* **119**, 246402 (2017).
- [43] W. A. Benalcazar, B. A. Bernevig, and T. L. Hughes, *Phys. Rev. B* **96**, 245115 (2017).
- [44] F. Schindler, A. M. Cook, M. G. Vergniory, Z. Wang, S. S. P. Parkin, B. A. Bernevig, and T. Neupert, *Science Advances* **4** (2018), 10.1126/sciadv.aat0346.
- [45] M. Ezawa, *Phys. Rev. Lett.* **120**, 026801 (2018).
- [46] X. Zhu, *Phys. Rev. B* **97**, 205134 (2018).
- [47] M. Geier, L. Trifunovic, M. Hoskam, and P. W. Brouwer, *Phys. Rev. B* **97**, 205135 (2018).
- [48] E. Khalaf, *Phys. Rev. B* **97**, 205136 (2018).
- [49] F. Schindler, Z. Wang, M. Vergniory, A. Cook, A. Murani, S. Sengupta, A. Kasumov, R. Deblock, S. Jeon, I. Drozdov, H. Bouchiat, S. Guéron, A. Yazdani, B. Bernevig, and T. Neupert, *Nature Physics* **14**, 918 (2018).
- [50] J. Bao, D. Zou, W. Zhang, W. He, H. Sun, and X. Zhang, *Phys. Rev. B* **100**, 201406 (2019).
- [51] J. Noh, W. A. Benalcazar, S. Huang, M. J. Collins, K. P. Chen, T. L. Hughes, and M. C. Rechtsman, *Nature Photonics* **12**, 408 (2018).
- [52] F. Zangeneh-Nejad and R. Fleury, *Phys. Rev. Lett.* **123**, 053902 (2019).
- [53] H. Fan, B. Xia, L. Tong, S. Zheng, and D. Yu, *Phys. Rev. Lett.* **122**, 204301 (2019).
- [54] H. Xue, Y. Yang, F. Gao, Y. Chong, and B. Zhang, *Nature Materials* **18**, 108 (2018).
- [55] X. Ni, M. Weiner, A. Alù, and A. Khanikaev, *Nature Materials* **18**, 113 (2019).
- [56] A. Hassan, F. Kunst, A. Moritz, G. Andler, E. Bergholtz, and M. Bourennane, *Nature Photonics* **13**, 697 (2019).
- [57] Y. Chen, X. Lu, and H. Chen, *Opt. Lett.* **44**, 4251 (2019).
- [58] M. Serra-Garcia, V. Peri, R. Süsstrunk, O. R. Bilal, T. Larsen, L. G. Villanueva, and S. D. Huber, *Nature* **555**, 342 (2018).
- [59] C. W. Peterson, W. A. Benalcazar, T. L. Hughes, and G. Bahl, *Nature* **555**, 346 (2018).
- [60] S. Imhof, C. Berger, F. Bayer, J. Brehm, L. W. Molenkamp, T. Kiessling, F. Schindler, C. H. Lee, M. Greiter, T. Neupert, and R. Thomale, *Nature Physics* **14**, 925 (2018).
- [61] S. Mittal, V. V. Orre, G. Zhu, M. A. Gorlach, A. Poddubny, and M. Hafezi, *Nature Photonics* **13**, 692 (2019).
- [62] M. Serra-Garcia, R. Süsstrunk, and S. D. Huber, *Phys. Rev. B* **99**, 020304 (2019).
- [63] X.-D. Chen, W.-M. Deng, F.-L. Shi, F.-L. Zhao, M. Chen, and J.-W. Dong, *Phys. Rev. Lett.* **122**, 233902 (2019).
- [64] B.-Y. Xie, G.-X. Su, H.-F. Wang, H. Su, X.-P. Shen, P. Zhan, M.-H. Lu, Z.-L. Wang, and Y.-F. Chen, *Phys. Rev. Lett.* **122**, 233903 (2019).
- [65] Y. Ota, F. Liu, R. Katsumi, K. Watanabe, K. Wakabayashi, Y. Arakawa, and S. Iwamoto, *Optica* **6**, 786

- (2019).
- [66] X. Zhang, H.-X. Wang, Z.-K. Lin, Y. Tian, B. Xie, M.-H. Lu, Y.-F. Chen, and J.-H. Jiang, *Nature Physics* **15**, 582 (2019).
- [67] D. Leykam, S. Mittal, M. Hafezi, and Y. D. Chong, *Phys. Rev. Lett.* **121**, 023901 (2018).
- [68] C. Poli, H. Schomerus, M. Bellec, U. Kuhl, and F. Mortessagne, *2D Materials* **4**, 025008 (2017).
- [69] M. Li, D. Zhirihin, M. Gorlach, X. Ni, D. Filonov, A. Slobozhanyuk, A. Alù, and A. Khanikaev, *Nature Photonics* **14**, 89 (2020).
- [70] D. Pozar, *Microwave Engineering, 4th Edition* (Wiley, 2011).
- [71] A. Wallraff, D. I. Schuster, A. Blais, L. Frunzio, R.-S. Huang, J. Majer, S. Kumar, S. M. Girvin, and R. J. Schoelkopf, *Nature* **431**, 162 (2004).
- [72] X. Gu, A. F. Kockum, A. Miranowicz, Y. X. Liu, and F. Nori, *Physics Reports* **718-719**, 1 (2017).
- [73] V. Peano, C. Brendel, M. Schmidt, and F. Marquardt, *Phys. Rev. X* **5**, 031011 (2015).